Shear and bulk viscosities of a gluon plasma in perturbative QCD: Comparison of different treatments for the $gg \leftrightarrow ggg$ process

Jiunn-Wei Chen,[1] Jian Deng,[2] Hui Dong,[2] and Qun Wang[3]

[1]*Department of Physics, Center for Theoretical Sciences, and Leung Center for Cosmology and Particle Astrophysics, National Taiwan University, Taipei 10617, Taiwan*

[2]*School of Physics, Shandong University, Shandong 250100, People's Republic of China*

[3]*Interdisciplinary Center for Theoretical Study and Department of Modern Physics, University of Science and Technology of China, Anhui 230026, People's Republic of China*

(Received 26 June 2012; published 22 February 2013)

The leading-order contribution to the shear and bulk viscosities, η and ζ, of a gluon plasma in perturbative QCD includes the $gg \leftrightarrow gg$ (22) process, $gg \leftrightarrow ggg$ (23) process, and multiple scattering processes known as the Landau-Pomeranchuk-Migdal (LPM) effect. Complete leading-order computations for η and ζ were obtained by Arnold, Moore, and Yaffe (AMY) and Arnold, Dogan, and Moore (ADM), respectively, with the inelastic processes computed by an effective $g \leftrightarrow gg$ gluon splitting. We study how complementary calculations with 22 and 23 processes and a simple treatment to model the LPM effect compare with the results of AMY and ADM. We find that our results agree with theirs within errors. By studying the contribution of the 23 process to η, we find that the minimum angle θ among the final-state gluons in the fluid local rest frame has a distribution that is peaked at $\theta \sim \sqrt{\alpha_s}$, analogous to the near-collinear splitting asserted by AMY and ADM. However, the average of θ is much bigger than its peak value, as its distribution is skewed with a long tail. The same θ behavior is also seen if the 23 matrix element is taken to the soft-gluon bremsstrahlung limit in the center-of-mass (CM) frame. This suggests that the soft-gluon bremsstrahlung in the CM frame still has some near-collinear behavior in the fluid local rest frame. We also generalize our result to a general SU(N_c) pure gauge theory and summarize the current viscosity computations in QCD.

DOI: 10.1103/PhysRevC.87.024910 PACS number(s): 25.75.Nq, 12.38.Mh

I. INTRODUCTION

Shear and bulk viscosities, η and ζ, are transport coefficients characterizing how fast a system returns to equilibrium under a shear mode perturbation and a uniform expansion, respectively. In a weakly interacting hot gluon plasma, η is inversely proportional to the scattering rate: $\eta \propto 1/\Gamma \propto 1/\alpha_s^2 \ln \alpha_s^{-1}$ [1], where α_s is the strong coupling constant. ζ is suppressed by an additional factor of $(T^\mu_\mu)^2$, arising from the response of the trace of the energy-momentum tensor (T^μ_μ) to a uniform expansion. Thus, ζ vanishes when the system is "conformal" or scale invariant. For a gluon plasma, the running of the coupling constant breaks the scale invariance. Thus, $T^\mu_\mu \propto \beta(\alpha_s) \propto \alpha_s^2$, $\zeta \propto \alpha_s^2/\ln \alpha_s^{-1}$ [2]. In the perturbative region, $\zeta/\eta \propto \alpha_s^4 \ll 1$.

In the strong-coupling region, smaller η is expected. The so-called perfect fluid is a fluid with the smallest shear viscosity per entropy density (s) ratio, η/s. It is conjectured that η/s has a minimum bound of $1/(4\pi)$ [3]. This is motivated by the uncertainty principle of quantum mechanics because η/s is related to $\Delta E \Delta t$, the product of the mean energy and lifetime of quasiparticles. The number $1/(4\pi)$ arises from the universal value $\eta/s = 1/(4\pi)$ obtained for a big class of strongly interacting conformal field theories (CFTs) in the large-N and large t'Hooft coupling limits, where N is the size of the gauge group [3–5]. This class of strongly interacting CFT's are dual to another class of weakly interacting gravitational theories in anti-de-Sitter space backgrounds. This anti-de-Sitter space/conformal field theory correspondence (AdS/CFT) [6–8] allow one to compute η/s in strongly interacting CFTs in weakly interacting gravitational theories.

The smallest η/s known so far is realized in the hot and dense matter (thought to be a quark gluon plasma of QCD) just above the phase transition temperature (T_c) produced at the Relativistic Heavy Ion Collider (RHIC) [9–11] with $\eta/s = 0.1 \pm 0.1(\text{theory}) \pm 0.08(\text{experiment})$ [12]. A robust upper limit of $\eta/s < 5 \times 1/(4\pi)$ was extracted by another group [13] and a lattice computation of gluon plasma yields $\eta/s = 0.102(56)$ (at temperature $T = 1.24T_c$) [14]. Away from T_c, η/s of QCD becomes larger due to small couplings at high T or small derivative Goldstone boson couplings at low T. We will summarize the current status of QCD η/s versus T in Fig. 7.

The bulk viscosity ζ is small in the perturbative region. However, near T_c, the rapid change of degrees of freedom gives a rapid change of T^μ_μ which could give very large ζ/s [15,16].

The best perturbative QCD calculation of ζ was carried out by Arnold, Dogan, and Moore (ADM) [2] using the same approach as used to compute η by Arnold, Moore, and Yaffe (AMY) in Refs. [1,17]. In both η and ζ, the leading-order (LO) contribution involves the elastic process $gg \leftrightarrow gg$ (22), inelastic number-changing process $gg \leftrightarrow ggg$ (23), and multiple scattering processes known as the Landau-Pomeranchuk-Migdal (LPM) effect. In the complete leading-order computations for η and ζ obtained by AMY and ADM, respectively, the inelastic processes were computed using an effective $g \leftrightarrow gg$ gluon splitting obtained after solving sophisticated integral equations.

In this paper, we study how complementary calculations with the 22 and 23 processes and a simple treatment to model

the LPM effect compare with the results of AMY and ADM. This approach is similar to the one used by Xu and Greiner (XG) [18,19], who claimed that the dominant contribution to η is 23 instead of 22, in sharp contradiction to the result of AMY. While our approach is not model independent due to our simplified treatment of the LPM effect, it can be used to double-check XG's result since the two approaches are very similar. We find that we cannot reproduce XG's result unless the 23 collision rate is at least multiplied by a factor of 6 (and part of this result was asserted in Ref. [20]). In the mean time, our η agrees with AMY's within errors, while our ζ also agrees with ADM's within errors.

Although our result does not provide a model-independent check to AMY's and ADM's results, we can still study the angular correlation between final-state gluons using our approach. Because the 23 matrix element that we use is exact in vacuum, we can check, modulo some model-dependent medium effect, whether the correlation is dominated by the near-collinear splitting as asserted by AMY and ADM.

We study the distribution of the minimum angle θ among the final-state gluons. If the near-collinear splittings dominate, then the most probable configurations would be that in which two gluons' directions are strongly correlated and their relative angle tends to be the smallest among the three relative angles in the final state. This can be seen most easily in the center-of-mass (CM) frame of the 23 collision with two gluons going along about the same direction while the third one is moving in the opposite direction. We expect it is also the case in the fluid local rest frame.

We find that the distribution of θ is peaked at $\theta \sim \sqrt{\alpha_s}$, analogous to the near-collinear splitting asserted by AMY and ADM. However, the average of θ, $\langle\theta\rangle$, is much bigger than its peak value, as its distribution is skewed with a long tail.

The same θ behavior is also seen if the 23 matrix element is taken to the soft-gluon bremsstrahlung limit in the CM frame. This suggests that the soft-gluon bremsstrahlung in the CM frame still has some near-collinear behavior in the fluid local rest frame.

We also generalize our result to a general SU(N_c) pure gauge theory and summarize the current viscosity computations in QCD.

II. KINETIC THEORY WITH THE 22 AND 23 PROCESSES

In this section, we will focus on the ζ computation. We refer the formulation for calculating η to Ref. [20].

By using the Kubo formula, ζ can be calculated through the linearized response function of a thermal equilibrium state $|\Omega\rangle$:

$$\zeta = \lim_{\omega\to 0}\frac{1}{9\omega}\int_0^\infty dt\int d^3x\, e^{i\omega t}\,\langle\Omega|\big[T^\mu_\mu(x),\, T^\nu_\nu(0)\big]|\Omega\rangle. \quad (1)$$

In the LO expansion of the coupling constant, the computation involves an infinite number of diagrams [21,22]. However, it is proven that the summation of the LO diagrams in a weakly coupled ϕ^4 theory [21–25] or in hot QED [26] is equivalent to solving the linearized Boltzmann equation with temperature-dependent particle masses and scattering amplitudes. This conclusion is expected to hold in perturbative QCD as well.

The Boltzmann equation of a hot gluon plasma describes the evolution of the color- and spin-averaged gluon distribution function $f_p(x)$, which is a function of space-time $x = (t, \mathbf{x})$ and momentum $p = (E_p, \mathbf{p})$.

The Boltzmann equation for the gluon plasma [27–32] reads

$$\begin{aligned}\frac{p^\mu}{E_p}\partial_\mu f_p = \frac{1}{N_g}\sum_{(n,l)}\frac{1}{N(n,l)}\int_{1\cdots(n-1)} d\Gamma_{1\cdots l\to(l+1)\cdots(n-1)p}\\ \times\left[(1+f_p)\prod_{r=1}^{l} f_r\prod_{s=l+1}^{n-1}(1+f_s)\right.\\ \left. - f_p\prod_{r=1}^{l}(1+f_r)\prod_{s=l+1}^{n-1} f_s\right]. \quad (2)\end{aligned}$$

The collision kernel

$$\begin{aligned}d\Gamma_{1\cdots l\to(l+1)\cdots(n-1)p} \equiv \prod_{j=1}^{n-1}\frac{d^3\mathbf{p}_j}{(2\pi)^3 2E_j}\frac{1}{2E_p}|M_{1\cdots l\to(l+1)\cdots(n-1)p}|^2\\ \times(2\pi)^4\delta^4\left(\sum_{r=1}^{l}p_r - \sum_{s=l+1}^{n-1}p_s - p\right) \quad (3)\end{aligned}$$

has summed over all colors and helicities of the initial and final states in the matrix element squared. $N_g = 2(N_c^2-1) = 16$ is the color ($N_c = 3$) and helicity degeneracy of a gluon. The ith gluon is labeled as i while the nth gluon is labeled as p. For a process with l initial and $(n-l)$ final gluons, the symmetry factor $N(n,l) = l!(n-l-1)!$. For example, processes $12\to 3p$, $12\to 34p$, and $123\to 4p$ yield $(n,l) = (4,2)$, $(5,2)$, and $(5,3)$ and $N(n,l) = 2$, 4, and 6, respectively. $|M_{1\cdots l\to(l+1)\cdots(n-1)p}|^2$ is the matrix element squared for the process $1\cdots l\to(l+1)\cdots(n-1)p$ without averaging over the degrees of freedom for incident gluons; i.e., it includes a factor N_g^2.

In vacuum, the matrix element squared for the 22 process is

$$|M_{12\to 34}|^2 = 8N_g(4\pi\alpha_s N_c)^2\left(3 - \frac{tu}{s^2} - \frac{su}{t^2} - \frac{st}{u^2}\right), \quad (4)$$

where $\alpha_s = g^2/(4\pi)$ is the strong coupling constant, and (s,t,u) are the Mandelstam variables $s = (p_1+p_2)^2$, $t = (p_1-p_3)^2$, and $u = (p_1-p_4)^2$.

For the 23 process [33–35], under the convention $\sum_{i=1}^5 p_i = 0$, we have

$$\begin{aligned}|M_{12345\to 0}|^2 &= |M_{0\to 12345}|^2\\ &= \frac{1}{10}N_g(4\pi\alpha_s N_c)^3[(12)^4+(13)^4\\ &\quad +(14)^4+(15)^4+(23)^4+(24)^4+(25)^4\\ &\quad +(34)^4+(35)^4+(45)^4]\\ &\quad \times\sum_{\mathrm{perm}\{1,2,3,4,5\}}\frac{1}{(12)(23)(34)(45)(51)}, \quad (5)\end{aligned}$$

where $(ij) \equiv p_i \cdot p_j$ and the sum is over all permutations (perm) of $\{1, 2, 3, 4, 5\}$. To convert to the convention $p_1 + p_2 = p_3 + p_4 + p_5$, we just perform the replacement

$$|M_{12\to345}|^2 = |M_{0\to12345}|^2|_{p_1\to-p_1,p_2\to-p_2},$$
$$|M_{345\to12}|^2 = |M_{12345\to0}|^2|_{p_1\to-p_1,p_2\to-p_2}. \tag{6}$$

In the medium, the gluon thermal mass serves as the infrared (IR) cutoff to regularize IR-sensitive observables. The most singular part of Eq. (4) comes from the collinear region (i.e., either $t \approx 0$ or $u \approx 0$), which can be regularized by the Hard Thermal Loop (HTL) corrections to the gluon propagators [36,37] and yields [38]

$$|M_{12\to34}|^2 \approx 4(4\pi\alpha_s N_c)^2 N_g (4E_1E_2)^2 \times \left|\frac{1}{\mathbf{q}^2+\Pi_L} - \frac{(1-\overline{x}^2)\cos\phi}{\mathbf{q}^2(1-\overline{x}^2)+\Pi_T}\right|^2, \tag{7}$$

where $q = p_2 - p_4 = (q_0, \mathbf{q})$, $\overline{x} = q_0/|\mathbf{q}|$, and ϕ is the angle between $\hat{\mathbf{p}}_1 \times \hat{\mathbf{q}}$ and $\hat{\mathbf{p}}_2 \times \hat{\mathbf{q}}$. The HTL self-energies Π_L (longitudinal) and Π_T (transverse) are given by

$$\Pi_L = m_D^2\left[1 - \frac{\overline{x}}{2}\ln\frac{1+\overline{x}}{1-\overline{x}} + i\frac{\pi}{2}\overline{x}\right],$$
$$\Pi_T = m_D^2\left[\frac{\overline{x}^2}{2} + \frac{\overline{x}}{4}(1-\overline{x}^2)\ln\frac{1+\overline{x}}{1-\overline{x}} - i\frac{\pi}{4}\overline{x}(1-\overline{x}^2)\right]. \tag{8}$$

The external gluon mass m_∞ (i.e., the asymptotic mass) is the mass for an on-shell transverse gluon. In both the HTL approximation and the full one-loop result, $m_\infty^2 = \Pi_T(|\overline{x}| = 1) = m_D^2/2$, where $m_D = (4\pi\alpha_s N_c/3)^{1/2}T$ is the Debye mass.

Previous perturbative analyses showed that the most important plasma effects are the thermal masses $\sim gT$ acquired by the hard thermal particles [39–41]. So a simpler (though less accurate) treatment for the regulator is to insert m_D into the gluon propagator such that

$$|M_{12\to34}|^2 \approx 8N_g(4\pi\alpha_s N_c s)^2\left[\frac{1}{\left(t-m_D^2\right)^2} + \frac{1}{\left(u-m_D^2\right)^2}\right]. \tag{9}$$

It can be shown easily that Eqs. (7) and (9) coincide in the CM frame in vacuum. This treatment was used in Refs. [18,29,42].

Equation (9) is often expressed in $\mathbf{q}_T$, the transverse component of $\mathbf{q}$ with respect to $\mathbf{p}_1$, in the CM frame. If we just include the final-state phase space of the t-channel, near-forward-angle scatterings ($\mathbf{q}^2 \approx \mathbf{q}_T^2 \approx 0$), then the backward angle contribution from the u channel can be included by multiplying the prefactor by a factor of 2:

$$|M_{12\to34}|^2_{\rm CM} \underset{\mathbf{q}^2\approx\mathbf{q}_T^2\approx0}{\approx} 16N_g(4\pi\alpha_s N_c)^2\frac{s^2}{\left(\mathbf{q}_T^2+m_D^2\right)^2}. \tag{10}$$

But if one includes the whole phase space in the calculation, then the factor of 2 is not needed:

$$|M_{12\to34}|^2_{\rm CM} \underset{\mathbf{q}_T^2\approx0}{\approx} 8N_g(4\pi\alpha_s N_c)^2\frac{s^2}{\left(\mathbf{q}_T^2+m_D^2\right)^2}. \tag{11}$$

Note that the constraint $\mathbf{q}^2 \approx 0$ is removed because both the near-forward and near-backward scatterings have small $\mathbf{q}_T^2$ but only the near-forward scatterings have small $\mathbf{q}^2$.

For the 23 process, because the matrix element is already quite complicated, we will just take m_D as the internal gluon mass as was done in the η computation in Ref. [20] and then estimate the errors. In the $\sum_{i=1}^5 p_i = 0$ convention, one can easily show that an internal gluon will have a momentum of $\pm(p_i + p_j)$ rather than $\pm(p_i - p_j)$. Therefore, the gluon propagator factors (ij) in the denominator of Eq. (5) are replaced by

$$(ij) = \frac{1}{2}\left[(p_i+p_j)^2 - m_D^2\right] = p_i\cdot p_j + \frac{2m_\infty^2 - m_D^2}{2} = p_i\cdot p_j. \tag{12}$$

Accidentally, $(ij) = p_i \cdot p_j$ is still correct after we have used the asymptotic mass for the external gluon mass. Then one applies Eq. (6) for the Boltzmann equation. In the numerator, the $(ij)^4$ combination is set by T and is $O(T^8)$. So we can still apply the substitution of Eq. (12), even if the (ij) factors might not have the inverse propagator form. The error is $\sim m_D^2(ij)^3 = O(\alpha_s T^8)$, which is higher order in α_s.

It is instructive to show that Eqs. (5), (6), and (12) give the correct soft bremsstrahlung limit. Using the light-cone variable

$$p = (p^+, p^-, \mathbf{p}_T) \equiv (p_0 + p_3, p_0 - p_3, p_1, p_2), \tag{13}$$

we can rewrite one momentum configuration in the CM frame in terms of p, p', q, and k: $p_1 = p$, $p_2 = p'$, $p_3 = p + q - k$, $p_4 = p' - q$, and $p_5 = k$, with

$$p = \left(\sqrt{s}, m_\infty^2/\sqrt{s}, 0, 0\right), \quad p' = \left(m_\infty^2/\sqrt{s}, \sqrt{s}, 0, 0\right),$$
$$k = \left(y\sqrt{s}, \left(k_T^2+m_\infty^2\right)/y\sqrt{s}, k_T, 0\right),$$
$$q = (q^+, q^-, \mathbf{q}_T). \tag{14}$$

The on-shell condition $p_3^2 = p_4^2 = m_\infty^2$ yields

$$q^+ \simeq -q_T^2/\sqrt{s},$$
$$q^- \simeq \frac{k_T^2 + yq_T^2 - 2y\mathbf{k}_T\cdot\mathbf{q}_T + (1-y+y^2)m_\infty^2}{y(1-y)\sqrt{s}}. \tag{15}$$

Here $y = k^+/p^+ = k_T e^z/\sqrt{s}$ is the light-cone momentum fraction of the bremsstrahlung gluon and z is its rapidity. In the central rapidity for the bremsstrahlung gluon, i.e. $z \sim 0$, y is toward zero. In this case $p_5 = k$ is very small compared to p_1 and p_2.

Now, in the limit $s \to \infty$, $y \to 0$, while keeping $y\sqrt{s}$ fixed, we have

$$p = (\sqrt{s}, 0, 0, 0), \quad p' = (0, \sqrt{s}, 0, 0),$$
$$k = \left(y\sqrt{s}, \left(k_T^2+m_\infty^2\right)/y\sqrt{s}, k_T, 0\right),$$
$$q = \left(0, \left(k_T^2+m_\infty^2\right)/y\sqrt{s}, \mathbf{q}_T\right). \tag{16}$$

In this limit, p_{1-4} are hard (their three-momenta are $O(\sqrt{s})$) while $q(=p_2 - p_4 = -p_1 + p_3 + p_5)$ and $p_5 = k$ are soft (their three-momenta are much smaller than $\sqrt{s}$). In this

particular limit of phase space, the matrix element becomes

$$|M_{12\to345}|^2_{\rm CM} \approx 32(4\pi\alpha_s N_c)^3 N_g \times \frac{s^2}{(k_T^2+m_\infty^2)(q_T^2+m_D^2)[(\mathbf{k}_T-\mathbf{q}_T)^2+m_D^2]}, \tag{17}$$

where the prefactor is equivalent to $3456\pi^3\alpha_s^3 N_g^2$ when $N_c = 3$. Note that there are six different permutations of (p_3, p_4, p_5), which give the same expression as Eq. (17) due to the permutation symmetry of Eq. (5). Those permutations correspond to different symmetric diagrams, just as the two permutations of (p_3, p_4) in Eq. (9) give the t- and u-channel diagrams by the crossing symmetry. Analogous to Eqs. (10) and (11), if we only include the constraint phase space of (p_3, p_4, p_5), then we need to multiple Eq. (17) by a factor of 6 to take into account the permutations of (p_3, p_4, p_5). But if we include all the phase space in the calculation, then Eqs. (5) and (6) have to be used. Any additional symmetry factor will result in multiple counting.

The ratio of Eq. (17) to Eq. (11) reproduces the Gunion-Bertsch (GB) formula [43] after taking $m_D, m_\infty \to 0$. One can find the derivation of the GB formula from Eq. (5) in Appendix A. One can also expand the "exact" matrix element in Eqs. (5) and (6) in terms of t/s to extend the GB formula [44–47].

An intuitive explanation of the LPM effect was given in Ref. [48]: for the soft bremsstrahlung gluon with transverse momentum k_T, the mother gluon has a transverse momentum uncertainty $\sim k_T$ and a size uncertainty $\sim 1/k_T$. It takes the bremsstrahlung gluon the formation time $t \sim 1/(k_T v_T) \sim E_k/{k_T}^2$ to fly far enough from the mother gluon to be resolved as a radiation. But if the formation time is longer than the mean free path $l_{\rm mfp} \approx O(\alpha_s^{-1})$, then the radiation is incomplete and it would be resolved as $gg \to gg$ instead of $gg \to ggg$. Thus, the resolution scale is set by $t \leqslant l_{\rm mfp}$. This yields an IR cutoff $k_T^2 \geqslant E_k/l_{\rm mfp} \approx O(\alpha_s)$ on the phase space [49]. Thus, the LPM effect reduces the 23 collision rate and will increase η and ζ. Our previous calculation of η using the Gunion-Bertsch formula shows that implementing the m_D regulator gives a result that is very close to the LPM effect [42]. Thus, we will estimate the size of the LPM effect by increasing the external gluon mass m_g from m_∞ to m_D.

III. AN ALGORITHM BEYOND VARIATION TO SOLVE FOR ζ

Following the derivation of Ref. [22], the energy-momentum tensor of the weakly interacting gluon plasma in kinetic theory can be modified as

$$T_{\mu\nu}(x) = N_g \int \frac{d^3\mathbf{p}}{(2\pi)^3 E_p} f_p(x)[p_\mu p_\nu - \Sigma(x) g_{\mu\nu}], \tag{18}$$

where $\Sigma(x)$ is an effective mass squared from the self-energy which encodes medium effects and $E_p = \sqrt{\mathbf{p}^2 + m_\infty^2}$. When the system deviates from thermal equilibrium infinitesimally, $f_p(x)$ deviates from its equilibrium value $f_p^{\rm eq} = (e^{v\cdot p/T} - 1)^{-1}$,

$$f_p = f_p^{\rm eq} + \delta f_p, \tag{19}$$

and so does $T_{\mu\nu}$,

$$\delta T_{\mu\nu} = N_g \int \frac{d^3\mathbf{p}}{(2\pi)^3 E_p} \delta f_p \left(p_\mu p_\nu - v_\mu v_\nu T^2 \frac{\partial m_\infty^2}{\partial T^2} \right), \tag{20}$$

where energy-momentum conservation $\partial^\mu T_{\mu\nu} = 0$ has been imposed.

In hydrodynamics, small deviations from thermal equilibrium can be systematically described by derivative expansions of hydrodynamical variables with respect to space-time. We will be working in the $\mathbf{v}(x) = 0$ frame for a specific space-time point x (i.e., the local fluid rest frame). This implies $\partial_\nu v^0 = 0$ after taking a derivative on $v_\mu(x)v^\mu(x) = 1$. Then energy-momentum conservation and thermal dynamic relations (where we have used the property that there is no conserved charge in the system) in equilibrium allow one to express the time derivatives $\partial_t T$ and $\partial_t \mathbf{v}$ in terms of the spacial derivatives $\nabla\cdot\mathbf{v}$ and ∇T. Thus, to the first derivative expansion of the hydrodynamical variables $\mathbf{v}$ and T, the bulk and shear viscosities are defined by the small deviation of $T_{\mu\nu}$ away from equilibrium:

$$\delta T_{ij} = -\zeta\delta_{ij}\nabla\cdot\mathbf{v} - \eta\left(\frac{\partial v^i}{\partial x^j} + \frac{\partial v^j}{\partial x^i} - \frac{2}{3}\delta_{ij}\nabla\cdot\mathbf{v}\right), \tag{21}$$

where i and j are spacial indexes. Also, $\delta T_{0i}(x) = 0$, since the momentum density at point x is zero in the local fluid rest frame, and one defines T_{00} to be the energy density in this frame. Therefore,

$$\delta T_{00} = 0 \ = N_g \int \frac{d^3\mathbf{p}}{(2\pi)^3 E_p} \delta f_p(\mathbf{p}^2 + \tilde{m}^2), \tag{22}$$

where

$$\tilde{m}^2 \equiv m_\infty^2 - T^2\frac{\partial m_\infty^2}{\partial T^2} = -\frac{1}{6}N_c\beta(g^2)T^2 = \frac{11}{18}N_c^2\alpha_s^2 T^2. \tag{23}$$

By matching kinetic theory [Eq. (20)] to hydrodynamics [Eq. (21)] to the first derivative order, δf_p can be parametrized as

$$\delta f_p = -\chi_p f_p^{\rm eq}(1 + f_p^{\rm eq}), \tag{24}$$

where

$$\chi_p = \frac{A(p)}{T}\nabla\cdot\mathbf{v} + \frac{B_{ij}(p)}{T}\frac{1}{2}\left(\frac{\partial v^i}{\partial x^j} + \frac{\partial v^j}{\partial x^i} - \frac{2}{3}\delta_{ij}\nabla\cdot\mathbf{v}\right). \tag{25}$$

We can further write $B_{ij}(p) = B(p)(\hat{\mathbf{p}}_i\hat{\mathbf{p}}_j - \frac{1}{3}\delta_{ij})$ with $\hat{\mathbf{p}}$ the unit vector in the $\mathbf{p}$ direction. $A(p)$ and $B(p)$ are functions of $\mathbf{p}$. They can be determined by the Boltzmann equation to give the solution of the bulk and shear viscosities, respectively. In this work, we will focus on solving the bulk viscosity.

Working to the first derivative order, the Boltzmann equation becomes a linear equation in δf_p, which

yields

$$\frac{\mathbf{p}^2}{3} - c_s^2(\mathbf{p}^2+\tilde{m}^2) = \frac{E_p}{2N_g}\int_{123} d\Gamma_{12\to 3p} f_1^{\rm eq} f_2^{\rm eq}\big(1+f_3^{\rm eq}\big)\big(f_p^{\rm eq}\big)^{-1}[A_3+A_p-A_1-A_2] + \frac{E_p}{4N_g}\int_{1234} d\Gamma_{12\to 34p} f_1^{\rm eq} f_2^{\rm eq}\big(1+f_3^{\rm eq}\big)\big(1+f_4^{\rm eq}\big)\big(f_p^{\rm eq}\big)^{-1}[A_3+A_4+A_p-A_1-A_2] + \frac{E_p}{6N_g}\int_{1234} d\Gamma_{123\to 4p} f_1^{\rm eq} f_2^{\rm eq} f_3^{\rm eq}\big(1+f_4^{\rm eq}\big)\big(f_p^{\rm eq}\big)^{-1}[A_4+A_p-A_1-A_2-A_3]. \tag{26}$$

Here we have used the notation $A_p \equiv A(p)$ and $A_i \equiv A(p_i)$ with $i = 1, 2, 3, 4$. The speed of sound squared, c_s^2, is defined as [2,22]

$$c_s^2 \equiv \frac{\partial P}{\partial \epsilon} = \frac{\int d^3p\, f_p^{\rm eq}\big(1+f_p^{\rm eq}\big)\mathbf{p}^2}{3\int d^3p\, f_p^{\rm eq}\big(1+f_p^{\rm eq}\big)(\mathbf{p}^2+\tilde{m}^2)}. \tag{27}$$

Then Eqs. (20), (21), and (25) yield

$$\zeta = \frac{N_g}{T}\int \frac{d^3p}{(2\pi)^3 E_p} f_p^{\rm eq}\big(1+f_p^{\rm eq}\big)\left[\frac{1}{3}\mathbf{p}^2 - c_s^2(\mathbf{p}^2+\tilde{m}^2)\right]A(p), \tag{28}$$

where we have added the c_s^2 term, which is proportional to $\delta T_{00} = 0$ for convenience. By substituting Eq. (26) into Eq. (28), we obtain

$$\zeta = \frac{1}{8T}\int \prod_{i=1}^{4}\frac{d^3k_i}{(2\pi)^3 2E_i}|M_{12\to 34}|^2(2\pi)^4\delta^4(E_1+E_2-E_3-E_4)\big(1+f_1^{\rm eq}\big)\big(1+f_2^{\rm eq}\big)f_3^{\rm eq}f_4^{\rm eq}[A_3+A_4-A_1-A_2]^2 + \frac{1}{12T}\int \prod_{i=1}^{5}\frac{d^3k_i}{(2\pi)^3 2E_i}|M_{12\to 345}|^2(2\pi)^4\delta^4(E_1+E_2-E_3-E_4-E_5)\big(1+f_1^{\rm eq}\big)\big(1+f_2^{\rm eq}\big) \times f_3^{\rm eq}f_4^{\rm eq}f_5^{\rm eq}[A_3+A_4+A_5-A_1-A_2]^2. \tag{29}$$

By the definition of c_s, the following integral vanishes:

$$\int \frac{d^3p}{(2\pi)^3 E_p} f_p^{\rm eq}\big(1+f_p^{\rm eq}\big)\left[\frac{\mathbf{p}^2}{3} - c_s^2(\mathbf{p}^2+\tilde{m}^2)\right]E_p = 0. \tag{30}$$

We will use this property later.

Now we first review the arguments that cast the computation of ζ as a variational problem [17,50]. Then we show how one can go beyond variation to find the answer systematically. Let us rewrite Eq. (26) schematically as

$$|S\rangle = C|A\rangle \tag{31}$$

and Eqs. (28) and (29) as

$$\zeta = \langle A|S\rangle = \langle A|C|A\rangle. \tag{32}$$

Note that Eq. (32) is just a projection of Eq. (31). Using $|A\rangle = C^{-1}|S\rangle$ from Eq. (31), we get

$$\zeta = \langle S|C^{-1}|S\rangle. \tag{33}$$

Technically, finding an ansatz $A_{\rm anz}$ that satisfies the projected equation $\langle S|A_{\rm anz}\rangle = \langle A_{\rm anz}|C|A_{\rm anz}\rangle$ of (32) is easier than solving the original integral equation (31). But this will not give the correct viscosity if $C|A_{\rm anz}\rangle \neq |S\rangle$. However, the resulting bulk viscosity is always less than the real one:

$$\begin{aligned}\zeta_{\rm anz} &= -\langle A_{\rm anz}|C|A_{\rm anz}\rangle + 2\langle A_{\rm anz}|S\rangle \\ &= -\langle A'_{\rm anz}|C|A'_{\rm anz}\rangle + \langle S|C^{-1}|S\rangle \\ &\leqslant \langle S|C^{-1}|S\rangle = \zeta,\end{aligned} \tag{34}$$

where $|A'_{\rm anz}\rangle \equiv |A_{\rm anz}\rangle - C^{-1}|S\rangle$ and $\langle A'_{\rm anz}|C|A'_{\rm anz}\rangle$ is real and non-negative. Thus, a variational calculation of ζ is possible: one just demands $\langle S|A_{\rm anz}\rangle = \langle A_{\rm anz}|C|A_{\rm anz}\rangle$ and tries to find the maximum $\zeta_{\rm anz}$. In what follows, we show an algorithm [see Eqs. (35)–(42)] that will approach the maximum $\zeta_{\rm anz}$ systematically.

We will choose a basis $\{\tilde{A}_i | i = 1, 2, \ldots, n\}$ with n orthonormal functions satisfying

$$\langle \tilde{A}_i|C|\tilde{A}_j\rangle = \delta_{ij}. \tag{35}$$

We impose the following condition for $\tilde{A}_i$:

$$\int \frac{d^3p}{(2\pi)^3 E_p} f_p^{\rm eq}\big(1+f_p^{\rm eq}\big)(\mathbf{p}^2+\tilde{m}^2)\tilde{A}_i(p) = 0, \tag{36}$$

and we take the following ansatz for A:

$$A_{\rm anz}^{(n)} \equiv \sum_{i=1}^{n} d_i \tilde{A}_i, \tag{37}$$

so that the constraint $\delta T_{00} = 0$ is automatically satisfied. Then Eq. (32) yields

$$\zeta_{\rm anz}^{(n)} = \sum_{i=1}^{n} d_i \langle \tilde{A}_i | S \rangle = \sum_{ij=1}^{n} d_i d_j \langle \tilde{A}_i | C | \tilde{A}_j \rangle = \sum_{i=1}^{n} d_i^2. \quad (38)$$

This equation does not determine d_i uniquely. However, what we want is the solution that maximizes $\zeta_{\rm anz}^{(n)}$, which is unique. It can be computed by rewriting Eq. (38) as

$$\begin{aligned}\zeta_{\rm anz}^{(n)} &= \sum_{i=1}^{n} \left(2 d_i \langle \tilde{A}_i | S \rangle - d_i^2\right) \\ &= \sum_{i=1}^{n} \langle \tilde{A}_i | S \rangle^2 - \sum_{i=1}^{n} (d_i - \langle \tilde{A}_i | S \rangle)^2. \end{aligned} \quad (39)$$

Then the solution

$$d_i = \langle \tilde{A}_i | S \rangle \quad (40)$$

satisfies the projected equation (38). It is also the solution we are looking for which maximizes $\zeta_{\rm anz}^{(n)}$. This solution yields

$$\zeta_{\rm anz}^{(n)} = \sum_{i=1}^{n} \langle \tilde{A}_i | S \rangle^2. \quad (41)$$

Since $\langle \tilde{A}_i | S \rangle$ is real, $\zeta_{\rm anz}^{(n)}$ is monotonically increasing with respect to n. Also, we have $\zeta \geqslant \zeta_{\rm anz}$ from Eq. (34). This yields

$$\zeta_{\rm anz}^{(n)} \leqslant \zeta_{\rm anz}^{(n+1)} \leqslant \zeta_{\rm anz}^{(n\to\infty)} = \zeta, \quad (42)$$

which means we can systematically approach ζ from below by increasing n, then we will see that $\zeta_{\rm anz}^{(n)}$ becomes larger and larger. We stop at a finite n when a good convergence of the series $\zeta_{\rm anz}^{(n)}$ is observed. So this algorithm systematically approaches ζ from below.

We will use the following basis:

$$\tilde{A}_i = \sum_{j=0}^{i} c_j (E_p/T)^j, \quad (43)$$

where $A_{\rm anz}^{(n)}$ is given by

$$A_{\rm anz}^{(n)} = \sum_{i=1}^{n} d_i \tilde{A}_i = \sum_{i=0}^{n} \tilde{c}_i (E_p/T)^i. \quad (44)$$

The orthonormal condition in Eq. (35) determines c_j and Eq. (40) determines d_i. Equivalently, one can also solve for $\tilde{c}_i$ directly by demanding that $\langle S | A_{\rm anz}^{(n)} \rangle = \langle A_{\rm anz}^{(n)} | C | A_{\rm anz}^{(n)} \rangle$ be satisfied and that the $\tilde{c}_i$ solution gives the maximum $\zeta_{\rm anz}^{(n)}$. Note that, although the E_p term does not contribute to $\langle A_{\rm anz}^{(n)} | C | A_{\rm anz}^{(n)} \rangle$ or $\langle S | A_{\rm anz}^{(n)} \rangle$, this does not mean that the c_1 coefficient is not fixed in this procedure. c_1 is fixed by the constraint $\delta T_{00} = 0$.

An alternative basis is used in Ref. [2]:

$$A_{\rm anz}^{\prime(n)} = \sum_{i=1}^{n} c_i' \frac{(p/T)^i}{(p/T+1)^{n-2}} + d' E_p. \quad (45)$$

The two bases give give consistent ζ. For example, at $\alpha_s = 0.1$, the agreement is better than 1% when we work up to $n = 6$.

IV. N_c SCALING AND NUMERICAL RESULTS

A. N_c scaling

Viscosities of a general SU(N_c) pure gauge theory can be obtained by simply rescaling the SU(3) result. By using the above formulas, it is easy to show that

$$\zeta = N_g g_1(\alpha_s N_c) T^3, \quad \eta = N_g g_2(\alpha_s N_c) T^3, \quad (46)$$

where g_1 and g_2 are dimensionless functions of $\alpha_s N_c$ only. This, together with $s \propto N_g$, yields

$$\frac{\zeta}{s} = h_1(\alpha_s N_c), \quad \frac{\eta}{s} = h_2(\alpha_s N_c), \quad (47)$$

where h_1 and h_2 are also dimensionless functions of $\alpha_s N_c$ only. Thus, our ζ/s, η/s and ζ/η versus $\alpha_s N_c$ curves in Fig. 6 are universal and suitable for a general SU(N_c) pure gauge theory. From now on, $N_c = 3$ unless otherwise specified. One can always rescale the results to an arbitrary N_c.

B. Leading-log result

As discussed above, in the leading-log approximation, one just needs to focus on the small q_T contribution from the 22 process while setting $c_0 = 0$. Furthermore, it was shown in [51,52] that using the HTL regulator (7) gives the same leading-log (LL) shear viscosity as that using the m_D regulator (9). For the bulk viscosity, this is also true. We obtained the same LL result as [2]:

$$\zeta_{\rm LL} \simeq 0.44 \frac{T^3 \alpha_s^2}{\ln(1/g)}. \quad (48)$$

This can be compared with [1,20]

$$\eta_{\rm LL} \simeq 0.17 \frac{T^3}{\alpha_s^2 \ln(1/g)}. \quad (49)$$

For a gluon plasma, we have

$$\frac{\zeta_{\rm LL}}{\eta_{\rm LL}} \simeq 2.6 \alpha_s^4 = 48\left(1/3 - c_s^2\right)^2. \quad (50)$$

This is parametrically the same as $\zeta/\eta = 15(1/3 - c_s^2)^2$ for the absorption and emission of light quanta (e.g., photons, gravitons, or neutrinos) by the medium [53]. In the $\alpha_s \ll 1$ region where QCD is perturbative, $\zeta \ll \eta$. Using the entropy density for noninteracting gluons, $s = N_g \frac{2\pi^2}{45} T^3$, we have

$$\frac{\zeta_{\rm LL}}{s} \simeq 0.063 \frac{\alpha_s^2}{\ln(1/g)}, \quad \frac{\eta_{\rm LL}}{s} \simeq \frac{0.025}{\alpha_s^2 \ln(1/g)}. \quad (51)$$

C. Numerical results of η and ζ

In our calculation, we use the HTL propagator for the 22 process. For the 23 process, for technical reasons, we use the internal gluon mass m_D instead of the HTL propagator in Eqs. (5)–(7) and (12), $E_p = \sqrt{\mathbf{p}^2 + m_\infty^2}$ in kinematics, and $f_p^{\rm eq}$ for the external gluon distribution. The errors from not implementing the HTL propagator in the 23 process and the modeling of the LPM effect and from the uncalculated $O(\sqrt{\alpha_s})$ higher order corrections are estimated in Appendix B.

In Fig. 1, we show our main result for the shear viscosity η in our previous paper [42], together with the theoretical error

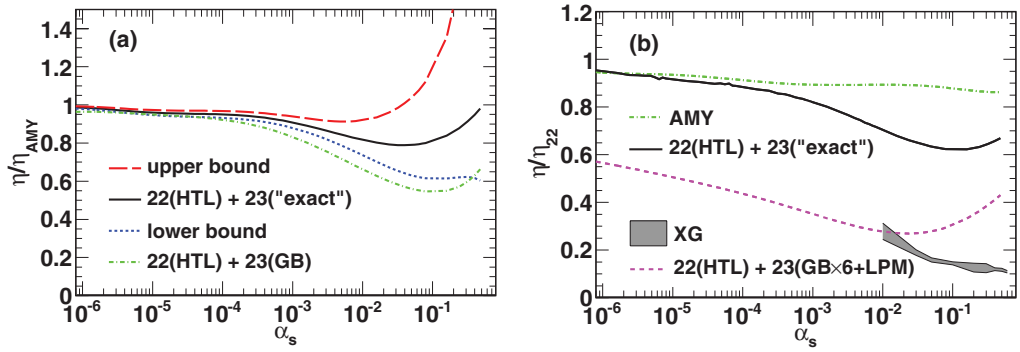

FIG. 1. (Color online) (a) The ratio of our numerical result (denoted as "exact") for the shear viscosity η to AMY's. The error is bounded by the upper and lower bounds. The result using the GB matrix element [Eq. (17)] is also shown. (b) Comparison of our result of η/η_{22} with those of AMY, XG, and "GB×6"(see the text). For our result the HTL gluon propagator is used for the 22 process, the "exact" matrix elements [Eqs. (5), (6), and (12)] are used for the 23 process, and the external gluon mass is set to m_∞. AMY's result is taken from Refs. [1,17] and XG's is from Ref. [19].

band bounded by "upper bound" and "lower bound" curves. Note that previously we estimated the higher order effect to be $O(\alpha_s)$ suppressed. But since the expansion parameter in finite-temperature field theory is g instead of g^2, we enlarge the error of the higher order effect to $O(\sqrt{\alpha_s})$ here. The result agrees with AMY's result within errors in Fig. 1(a) although our central value is lower at larger α_s. If we replace the "exact" matrix element of Eqs. (5)–(7) and (12) by the GB matrix element of Eq. (17), then η is reduced but still close to the estimated lower bound. This means that the 23 collision rate in GB is bigger than that in "exact."

The effect of the 23 process can be seen more clearly in the ratio η/η_{22} (where η_{22} means the shear viscosity with the 22 process included only) shown in Fig. 1(b), where we also show AMY's and XG's results for comparison. In AMY's result [1,17], the near-collinear $1 \leftrightarrow 2$ process gives η/η_{22} close to unity. This implies that their 12 collision is just a small perturbation to the 22 rate. However, XG employ the soft-gluon bremsstrahlung approximation in the matrix element for the 23 process, getting $\eta/\eta_{22} \simeq 0.11$–$0.16$ (around 1/8) in Ref. [18], indicating that their 23 collision rate is about 7 times the 22 one. In their improved treatment using the Kubo relation [19], they get $\eta/\eta_{22} \simeq 0.1$–$0.3$, indicating that the 23 collision rate is about 2–9 times the 22 rate.

Our central result lies between AMY's and XG's results. However, even given the lower bound, our 23 rate does not get bigger than the 22 rate. Thus, it is qualitatively consistent with AMY's result but inconsistent with XG's result. When compared with AMY's result, in addition to the error band shown in Fig. 1(a), there is still ∼10% difference at $\alpha_s = 0.01$. This is consistent with the $\sim m_g^2/T^2$ effect from using different inputs for external gluon mass—we use m_g while AMY use zero.

We find that we cannot reproduce XG's result unless we use a 23 matrix element squared at least 6 times larger. To compare with XG's calculation, we use the same $m_\infty = 0$ and LPM effect as XG, and

$$|M_{12\to345}|^2_{\rm CM} \to 6\times 54 g^6 N_g^2 \frac{q_T^2 s^2}{k_T^2\left(q_T^2+m_D^2\right)^2\left[(\mathbf{k}_T-\mathbf{q}_T)^2+m_D^2\right]}, \quad (52)$$

which is a slightly different variation of the GB matrix element squared of Eq. (17) multiplied by a factor of 6 (denoted as "GB×6"). This reproduces XG's result at $\alpha_s = 0.01$. The origin of this discrepancy is yet to be resolved.

In Fig. 2, η/s with various inputs are shown. At $\alpha_s = 0.3$ and 0.6, the GB×6 curve yields $\eta/s = 0.19$ and 0.09, respectively, while XG has 0.13 and 0.08. The central value of the "exact" result is about twice as large.

Our result for the bulk viscosity ζ using the "exact" matrix element for the 23 process is shown in Fig. 3. We have worked up to $n = 6$ and seen good convergence. For example, we obtain $\zeta^{(n)}_{\rm anz} \sim 95\%$, 98%, and 99.5% of $\zeta^{(6)}_{\rm anz}$ at $\alpha_s = 10^{-4}$ for $n = 3$, 4, and 5, respectively. The convergence for larger α_s is even better. When $\alpha_s \lesssim 10^{-8}$, our result approaches the LL one. At larger α_s, the 23 process becomes more important such that when $\alpha_s \gtrsim 0.1$, ζ is saturated by the 23 contribution [see Fig. 3(b)]. Our result agrees with that of ADM [2] in the full range of α_s within the error band explained in Appendix B.

D. Angular correlation in the 23 process

As mentioned in Sec. I, although our result does not provide a model-independent check to AMY's and ADM's results, we can still study the angular correlation between final-state

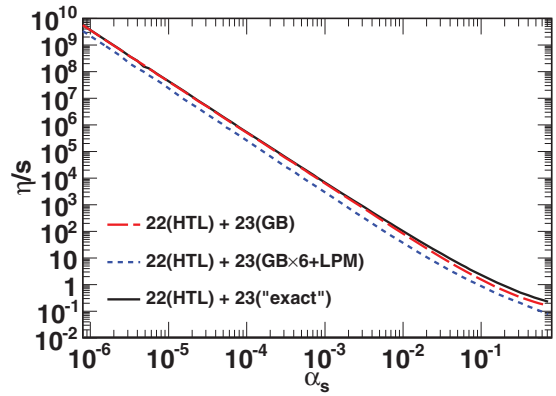

FIG. 2. (Color online) η/s with various inputs.

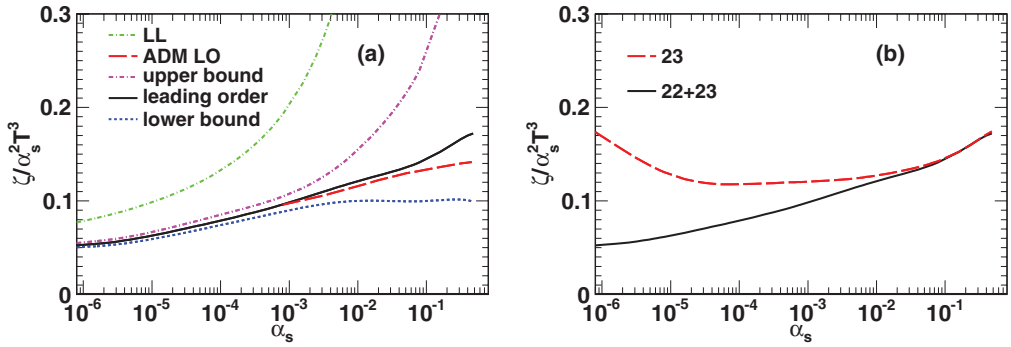

FIG. 3. (Color online) (a) Comparison of our result for the bulk viscosity ζ and its error band (see Appendix B) with ADM's result. "LL" denotes the leading-log result of Eq. (48). "ADM LO" denotes ADM's leading-order result read off from Ref. [2] (only available for $\alpha_s \gtrsim 8 \times 10^{-4}$). (b) Our full result for ζ (denoted as $22+23$) and ζ with the 23 process only (denoted as 23).

gluons using our approach. Because the 23 matrix element that we use is exact in vacuum, we can check, modulo some model-dependent medium effect, whether the correlation is dominated by the near-collinear splittings as asserted by AMY and ADM.

We study the distribution of the minimum angle θ among the final-state gluons. If the near-collinear splittings dominate, then the most probable configuration would be that in which two gluons have angles that are strongly correlated and their relative angle tends to be the smallest among the three relative angles in the final state. This can be seen most easily in the CM frame of the 23 collision with two gluons going along about the same direction while the third one is moving in the opposite direction. We expect it is also the case in the fluid local rest frame.

We find that the distribution of θ is peaked at $\theta^{\rm peak} \sim \sqrt{\alpha_s}$, analogous to the near-collinear splitting asserted by AMY and ADM. However, the average of θ, $\langle\theta\rangle$, is much bigger than its peak value, as its distribution is skewed with a long tail. Below are more detailed descriptions of our results.

We show the distribution of θ in the fluid local rest frame in Fig. 4, and we show the distribution in the CM frame of the 23 collision in Fig. 5. In both figures, the left panel is the distribution weighted by the phase space and the Bose-Einstein distribution functions, the middle panel is weighted by the 23 contribution to η [denoted as η_{23}, which is the η analogy of the second term in Eq. (29)] with the "exact" matrix element, and the right panel is similar to the middle one with the GB matrix element.

We first look at the distribution in the fluid local rest frame in Fig. 4. The left panel plots do not depend on the interaction and hence are α_s independent. The distribution has $\theta^{\rm peak} \simeq \langle\theta\rangle$ and the variation σ_θ is about the same size. In the middle panel, the η_{23}-weighted distribution with the "exact" matrix element, on the other hand, has $\theta^{\rm peak} \sim \sqrt{\alpha_s}$ at small α_s, while $\langle\theta\rangle$ is significantly bigger and σ_θ is close to its value in the left panel. In the right panel, where the GB matrix element is used, $\theta^{\rm peak}$

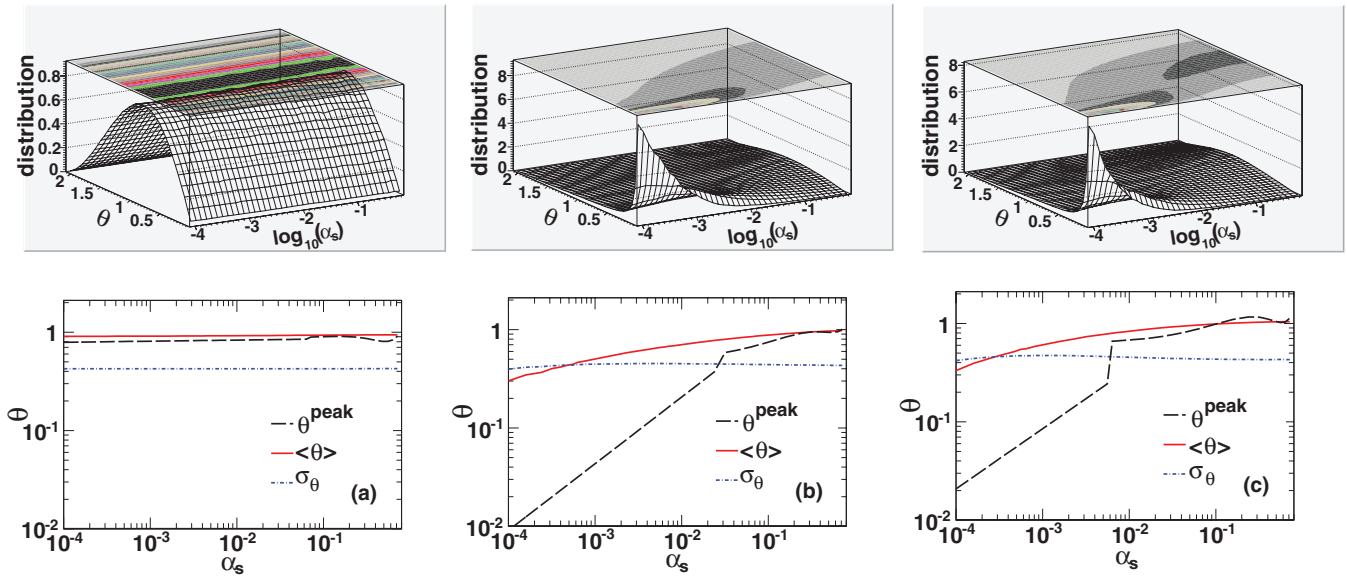

FIG. 4. (Color online) The distribution of θ in the fluid local rest frame, (a) weighted by the phase space and the Bose-Einstein distribution functions only, (b) weighted by the contribution to η_{23} with the "exact" matrix element, and (c) weighted by the contribution to η_{23} with the GB matrix element. The upper panels are normalized to unity for each coupling constant. The lower panels show the location of the peak $\theta^{\rm peak}$, the average value $\langle\theta\rangle$, and the variation σ_θ of the angle. The angle is in units of radians.

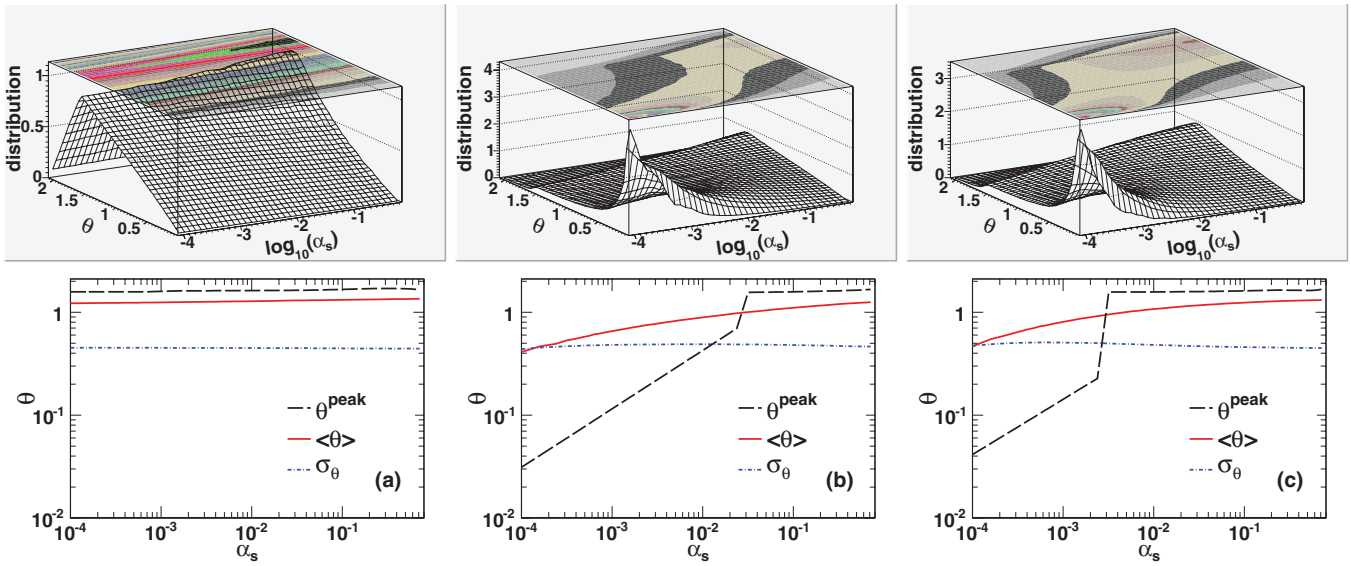

FIG. 5. (Color online) Same as Fig. 4 but with θ in the CM frame.

is still close to being proportional to $\sqrt{\alpha_s}$ at small α_s, but the angle is about twice as big as the "exact" case.

The distribution in the 23 collision CM frame shown in Fig. 5 has a behavior similar to that in the fluid local rest frame but the angles are in general much larger.

The above analysis suggests that the GB formula, which takes the soft-gluon bremsstrahlung limit in the CM frame, still has some near-collinear splitting behavior in the fluid local rest frame. It is curious what the nature of the long tail is. We will leave it for future investigation.

E. More aspects

Our results for ζ/s and η/s (where η/s is computed in Ref. [20]) using the "exact" matrix element for the 23 process are shown in Fig. 6(a) and their ratio ζ/η in units of α_s^4 and $(1/3 - c_s^2)^2$ are shown in Fig. 6(b). As we emphasize in Sec. IV A, these are universal curves suitable for a general SU(N_c) pure gauge theory.

The external gluon mass m_∞ is included in the entropy density s here, but it is a higher order effect and numerically very small at small α_s. In the range where perturbation theory is reliable ($\alpha_s \lesssim 0.1$), ζ is always smaller than η by at least three orders of magnitude. One can see that our result of ζ/η agrees with the $15(1/3 - c_s^2)^2$ result of Weinberg parametrically [53], and it is rather close to the LL one in Eq. (50).

In Fig. 7, we have plotted η/s and ζ/s versus T/T_c for QCD with various numbers of light quark flavors, N_f (with different T_c's used in different systems), at zero baryon chemical potential. In η/s, with $T/T_c \ll 1$, the QCD result is calculated by the pion gas system using the Boltzmann equation [54]. (The kaon mass is more than twice T_c—too heavy to be important for $T/T_c \ll 1$; for other calculations in hadronic gases, see [55–59]). The $T/T_c \gtrsim 1$ result is for gluon plasma using lattice QCD (LQCD) [14,60,61] (see [62] for a recent review; for a lattice-inspired model around T_c, see, e.g., Ref. [63]). This result is based on an assumed certain functional form for the spectral function and hence has some model dependence. Note that, in this temperature region, there might be anomalous shear viscosity arising from coherent color fields in the early stage of the quark gluon plasma [64]. We have also shown the value of η/s extracted

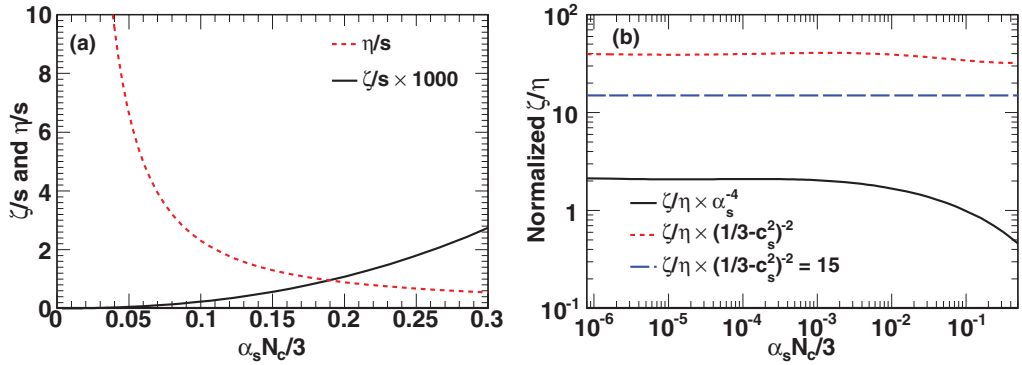

FIG. 6. (Color online) Universal curves for ζ/s (this work), η/s [20], and their ratio. These curves are universal and suitable for a general SU(N_c) pure gauge theory.

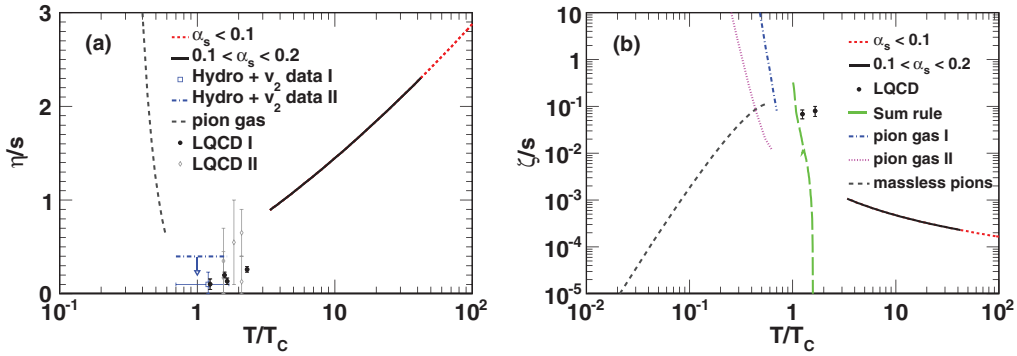

FIG. 7. (Color online) (a) η/s for a pion gas [54] and a gluon plasma with LQCD [14,60,61] and perturbative QCD [20], together with η/s extracted from RHIC elliptical flow (v_2): I [12] and II [13]. The arrow below the line of "Hydro + v_2 data II" indicates that it is an upper bound. (b) ζ/s for a massive [69,70] and massless [54] pion gas and a gluon plasma with LQCD [76] and perturbative QCD (this work). The sum-rule result [16] is for $N_f = 3$. The massive pion curves are denoted as "pion gas I" (inelastic process [69]) and "pion gas II" (elastic process [70]).

from the elliptic flow (v_2) data of RHIC using hydrodynamics: $\eta/s = 0.1 \pm 0.1(\text{theory}) \pm 0.08(\text{experiment})$ [12] (denoted as "Hydro+v_2 data I") and $\eta/s < 5 \times 1/(4\pi)$ [13] (denoted as "Hydro+v_2 data II"). And we have assigned a conservative temperature range $T = 0.24 \pm 0.10$ GeV that covers the initial and final temperatures in the hydrodynamic evolution ($T_f = 0.14$ GeV, $T_i \lesssim 0.34$ GeV).

For $T/T_c \gg 1$, we use the perturbative result of the gluon plasma with the 22 and 23 processes in the Boltzmann equation [20] and the standard two-loop renormalization (but the scheme dependence is of higher order) for the SU(3) pure gauge theory,

$$\frac{1}{4\pi\alpha_s(T)} = 2\beta_0 \ln\left(\frac{\mu T}{\Lambda_{\overline{MS}}}\right) + \frac{\beta_1}{\beta_0}\ln\left[2\ln\left(\frac{\mu T}{\Lambda_{\overline{MS}}}\right)\right], \quad (53)$$

where $\beta_0 = 11/(16\pi^2)$ and $\beta_1 = 102/(16\pi^2)^2$. Fitting to lattice data at $1.2 \lesssim T/T_c \lesssim 2$ yields $\mu \simeq 1.14\pi$, $\Lambda_{\overline{MS}} \simeq 261$ MeV, and $T_c \simeq 202$ MeV [65]. When $T/T_c \simeq 3.3$ and 42, $\alpha_s = 0.2$ and 0.1, respectively. If η/s above T_c is dominated by the gluon contribution so that the gluon plasma result ($N_f = 0$) is close to that of $N_f = 3$ QCD,[1] then Fig. 7 shows that η/s might have a local minimum at T_c [54,66,67].

For ζ/s with $T/T_c \ll 1$, the QCD result is calculated by using the Boltzmann equation for massless [68] and massive [69,70] (also in Refs. [71,72]) pions. For massless pions, ζ/s is increasing in T since it is expected that, when the pion self-coupling vanishes (or, equivalently, the pion decay constant $f_\pi \to \infty$), ζ also vanishes. Thus, the dimensionless combination $\zeta/s \propto (T/f_\pi)^z$, where z is some positive number. For massive pions, the expected nonrelativistic limit for the bulk viscosity reads [70] $\zeta \sim f_\pi^4\sqrt{T}/m_\pi^{3/2}$, where $m_\pi = 138$ MeV is the physical pion mass and one uses Weinberg's low-energy result for the pion-pion cross section at low energy (low temperature) [71]. This suggests that (nonrelativistic) conformal symmetry is recovered at zero T when particle number conservation is imposed. In the relativistic case, in Ref. [69] it is argued that the number-changing process (the 24 process, since 23 not allowed by parity conservation) is slower than 22, so it controls the time scale for the system to return to thermal equilibrium. At low enough T, this time scale is very long since there are not many pions energetic enough to collide and produce four pions. However, if the time scale is longer than that of the fireball expansion at RHIC, the elastic scattering [55,70,73] (see also [74,75]) is more relevant phenomenologically. For $T/T_c \gtrsim 1$, a LQCD calculation of a gluon plasma has been shown [76] together with the sum-rule result with $N_f = 3$ [15,16]. Both of them have some model dependence on the shape of the spectral function used. This issue was discussed extensively in Refs. [77–79], which inspired the author of Ref. [76] to include a delta function contribution to the spectral function, which was missed in the earlier result of Ref. [80]. The same delta function will modify the sum-rule result [15,16] as well. This is yet to be worked out.

For $T/T_c \gg 1$, the perturbative result of the gluon plasma calculated in this work is shown. We see that, although ζ/s for the massive pion case is decreasing in T for small T, it should merge to the massless pion result when the pion thermal energy $\sim 3T$ is greater than m_π. Thus, it is still possible that ζ/s has a local maximum at T_c as in some model calculations [67,81,82], provided there is not much difference between the $N_f = 0$ and $N_f = 3$ results above T_c.

It is very interesting that $\zeta > \eta$ for the gluon plasma just above T_c. This suggests that a fluid could still be perfect without being conformal, like the AdS/CFT model of Ref. [81]. Finally, it is intriguing that η/s might have a local minimum at T_c and ζ/s might have a local maximum at T_c. However, despite many other systems exhibiting this behavior for η/s [58,66,83,84], there are counterexamples showing that it is not universal [85–88].

[1] It is curious how to compute η/s below T_c for $N_f = 0$ and 1. There is no Goldstone mode in this case and there is no obvious gap in the spectrum to justify an effective field theory treatment. The lattice QCD computation also suffers from small correlator signals due to heavy hadron masses in the intermediate states.

V. CONCLUSIONS

We have calculated the shear and bulk viscosity of a weakly interacting gluon plasma with 22 and 23 collisional processes and a simple treatment to model the LPM effect. Our results agree with the results of AMY and ADM within errors. By studying the 23 contribution to η, we find that the minimum angle θ among the final-state gluons has a distribution that is peaked at $\theta \sim \sqrt{\alpha_s}$, analogous to the near-collinear splitting asserted by AMY and ADM. However, the average of θ is much bigger than its peak value, as its distribution is skewed with a long tail, which is worth further exploration. The same θ behavior is also seen if the 23 matrix element is taken to the soft-gluon bremsstrahlung limit in the CM frame. This suggests that the soft-gluon bremsstrahlung in the CM frame still has some near-collinear behavior in the fluid local rest frame. We also generalize our result to a general SU(N_c) pure gauge theory and summarize the current theoretical results for viscosities in QCD.

ACKNOWLEDGMENTS

Q.W. thanks C. Greiner for bringing our attention to their latest results about the shear viscosity for the 23 process. We thank G. Moore for useful communications related to his work. J.W.C. thanks INT, Seattle, for hospitality. J.W.C. is supported by the NSC, NCTS, and CASTS of ROC. Q.W. is supported in part by the National Natural Science Foundation of China (NSFC) under Grants No. 10735040 and No. 11125524. H.D. is supported in part by the NSFC under Grant No. 11105084 and the Natural Science Foundation of the Shandong province under Grant No. ZR2010AQ008. JD is supported in part by the NSFC under Grant No. 11105082 and the Innovation Foundation of Shandong University under Grant No. 2010GN031.

APPENDIX A: SOFT-GLUON BREMSSTRAHLUNG

In this Appendix, we give the details of the derivation of the GB formula or the matrix element for the soft-gluon bremsstrahlung. We work in the CM frame of the initial or final state where the longitudinal direction is defined as that of $\mathbf{p}_1$ or $\mathbf{p}_2$. The conditions for the soft-gluon bremsstrahlung are $s \gg p_{iT}$ and $k_T \gg yq_T$ (or $s \to \infty$ and $y \to 0$). This means that the energy of the bremsstrahlung gluon, say E_5, is much smaller than the other two gluons, $E_5 \ll E_3, E_4$.

It is convenient to use the Mandelstam-like variables defined as

$$\begin{aligned} &s = (p_1+p_2)^2, \quad t = (p_1-p_3)^2, \quad u = (p_1-p_4)^2,\\ &s' = (p_3+p_4)^2, \quad t' = (p_2-p_4)^2, \quad u' = (p_2-p_3)^2,\\ &T_{i5} = (k_i+k_5)^2 \ \ (i=1,2,3,4). \end{aligned} \tag{A1}$$

Here we assume all gluons are massless, so we obtain

$$\begin{aligned} &(12) = \frac{s}{2}, \quad (13) = -\frac{t}{2}, \quad (14) = -\frac{u}{2}, \quad (23) = -\frac{u'}{2},\\ &(24) = -\frac{t'}{2}, \quad (34) = \frac{s'}{2}, \quad (15) = \frac{T_{15}}{2},\\ &(25) = \frac{T_{25}}{2}, \quad (35) = \frac{T_{35}}{2}, \quad (45) = \frac{T_{45}}{2}. \end{aligned} \tag{A2}$$

Using light-cone variables in Eq. (13) and taking the limit $s \to \infty$ or $s \gg p_{iT}^2$, we have

$$\begin{aligned} &t = -\frac{1}{1-y}(\mathbf{q}_T - \mathbf{k}_T)^2, \quad u \approx -s, \quad s' \approx (1-y)s,\\ &t' = -q_T^2, \quad u' = -(1-y)s, \quad T_{15} \approx k_T^2/y, \quad T_{25} \approx ys,\\ &T_{35} \approx \frac{(\mathbf{k}_T - y\mathbf{q}_T)^2}{(1-y)y}, \quad T_{45} \approx ys. \end{aligned} \tag{A3}$$

We see that t, t', and T_{i5} $(i = 1, 2, 3, 4)$ are small. In evaluating $|M_{12\to345}|^2$, we denote $(12345) \equiv 1/[(12)(23)(34)(45)(51)]$, and we can evaluate all quantities in the denominator of Eq. (5),

$$\begin{aligned} &(12345) = -\frac{1}{su's'T_{15}T_{45}}, \quad (12354) = \frac{1}{su'uT_{35}T_{45}},\\ &(12435) = -\frac{2^5}{ss't'T_{15}T_{35}}, \quad (12453) = \frac{1}{stt'T_{35}T_{45}},\\ &(12534) = -\frac{1}{ss'uT_{25}T_{35}}, \quad (12543) = -\frac{1}{ss'tT_{25}T_{45}},\\ &(13245) = -\frac{1}{u'tt'T_{15}T_{45}}, \quad (13254) = -\frac{1}{uu'tT_{25}T_{45}},\\ &(13425) = \frac{1}{s'tt'T_{15}T_{25}}, \quad (13524) = -\frac{1}{utt'T_{25}T_{35}},\\ &(14235) = -\frac{1}{uu't'T_{15}T_{35}}, \quad (14325) = \frac{1}{uu's'T_{15}T_{25}}, \end{aligned} \tag{A4}$$

where we have factored out 2^5. Note that other permutations which do not appear are given by the identity $(12345) = (15432)$. Then we can collect the most singular parts involving t, t', and T_{i5} $(i = 1, 2, 3, 4)$ in the denominator and obtain

$$\begin{aligned} |M_{12\to345}|^2 &\sim \frac{1}{stt'T_{35}T_{45}} - \frac{1}{u'tt'T_{15}T_{45}} + \frac{1}{s'tt'T_{15}T_{25}}\\ &\quad - \frac{1}{utt'T_{25}T_{35}} - \frac{1}{ss't'T_{15}T_{35}} - \frac{1}{ss'tT_{25}T_{45}}\\ &\quad - \frac{1}{uu'tT_{25}T_{45}} - \frac{1}{uu't'T_{15}T_{35}}\\ &\sim \frac{2}{s^2q_T^2}\left[\frac{1}{(\mathbf{q}_T-\mathbf{k}_T)^2}\frac{(1-y)^2}{(\mathbf{k}_T-y\mathbf{q}_T)^2}\right.\\ &\quad \left. + \frac{1}{(\mathbf{q}_T-\mathbf{k}_T)^2}\frac{1}{k_T^2} + \frac{y^2}{(\mathbf{k}_T-y\mathbf{q}_T)^2k_T^2}\right]. \end{aligned} \tag{A5}$$

One can see that the matrix element squared has singularities from three poles at $k_T^2 = 0$, $(\mathbf{q}_T - \mathbf{k}_T)^2 = 0$. For the soft limit, $k_T \gg yq_T$, this can be realized by setting $y \to 0$, and we obtain

$$|M_{12\to345}|^2_{\text{soft}} \sim \frac{4}{s^2q_T^2}\frac{1}{(\mathbf{q}_T-\mathbf{k}_T)^2k_T^2}, \tag{A6}$$

which reproduces the GB formula.

APPENDIX B: ERROR ESTIMATION

The error bands of η and ζ shown in Figs. 1 and 3 are based on the estimation of the following errors:

(i) HTL corrections for the 23 process: In the 22 process, if we replace the HTL scattering amplitude of Eq. (7) by that of Eq. (9) with m_D as the regulator, then the 22 collision rate is reduced by $\sim$30% for $\alpha_s \simeq 0.005$–0.1. At smaller α_s, the effect becomes smaller and eventually becomes negligible at $\alpha_s = 10^{-8}$. The reduction arises because the HTL magnetic screening effect gives a smaller IR cutoff than m_D. Analogously, using m_D as the regulator in the 23 process tends to underestimate the 23 collision rate and gives a larger η and ζ.

(ii) The LPM effect: Our previous calculation on η using the Gunion-Bertsch formula shows that implementing the m_D regulator gives a result that is very close to the LPM effect [42]. Thus, we will estimate the size of the LPM effect by increasing the external gluon mass m_g from m_∞ to m_D.

(iii) The higher order effect: The higher order effect is parametrically suppressed by $O(\sqrt{\alpha_s})$, but the size is unknown. Computing this effect requires a treatment beyond the Boltzmann equation [25] and the inclusion of the 33 and 24 processes. We just estimate the effect to be $\sqrt{\alpha_s}$ times the leading order, which is $\sim$10% at $\alpha_s = 0.01$. (Note that we estimated the higher order effect to be $O(\alpha_s)$ suppressed in Ref. [42]. But since the expansion parameter in finite-temperature field theory is g instead of g^2, we enlarge the error here.)

Combining the above analyses, we consider errors from (i) to (iii). To compute a recommended range of ζ (and the range of η is computed analogously), we will work with the R_{22} and R_{23} collision rates defined as

$$R_{23}^{-1} \equiv \zeta_{23}, \quad (R_{22} + R_{23})^{-1} \equiv \zeta_{22+23}, \tag{B1}$$

where ζ_{23} is the bulk viscosity for a collision with the 23 process only. Using HTL instead of m_D for the gluon propagator enhances the 22 rate by a factor of

$$\delta \equiv \frac{R_{22(\mathrm{HTL})}}{R_{22(\mathrm{MD})}}. \tag{B2}$$

We will assume that the same enhancement factor appears in the 23 rate as well, such that

$$\frac{R_{23(\mathrm{HTL})}}{R_{23(\mathrm{MD})}} \simeq \delta. \tag{B3}$$

On the other hand, the LPM effect is estimated to suppress the 23 rate by a factor of

$$\gamma = \frac{R_{23(\mathrm{LPM})}}{R_{23(\mathrm{MD})}}. \tag{B4}$$

Combining the estimated HTL and LPM corrections to the 23 rate, the $22+23$ rate is likely to be in the range $[R_{22} + R_{23}, R_{22} + \gamma\delta R_{23}]$, while the higher order effect gives $\pm\sqrt{\alpha_s}(R_{22} + R_{23})$ corrections to the rate. Without further information, the errors are assumed to be Gaussian and uncorrelated, so the total rate is

$$\left(R_{22} + \frac{\gamma\delta + 1}{2} R_{23}\right) \pm \left(\frac{\gamma\delta - 1}{2} R_{23}\right) \pm \sqrt{\alpha_s}(R_{22} + R_{23}), \tag{B5}$$

and the recommended upper (ζ_+) and lower (ζ_-) ranges for ζ are

$$\zeta_\pm = \frac{1}{\left(R_{22} + \frac{\gamma\delta+1}{2} R_{23}\right) \mp \sqrt{\left(\frac{\gamma\delta-1}{2} R_{23}\right)^2 + \alpha_s (R_{22} + R_{23})^2}}. \tag{B6}$$

The $\zeta_\pm$ values are shown in the left panel of Fig. 3.

[1] P. Arnold, G. D. Moore, and L. G. Yaffe, J. High Energy Phys. 11 (2000) 001.
[2] P. B. Arnold, C. Dogan, and G. D. Moore, Phys. Rev. D **74**, 085021 (2006).
[3] P. K. Kovtun, D. T. Son, and A. O. Starinets, Phys. Rev. Lett. **94**, 111601 (2005).
[4] A. Buchel and J. T. Liu, Phys. Rev. Lett. **93**, 090602 (2004).
[5] A. Buchel, Phys. Lett. B **609**, 392 (2005).
[6] J. M. Maldacena, Adv. Theor. Math. Phys. **2**, 231 (1998); Int. J. Theor. Phys. **38**, 1113 (1999).
[7] S. S. Gubser, I. R. Klebanov, and A. M. Polyakov, Phys. Lett. B **428**, 105 (1998).
[8] E. Witten, Adv. Theor. Math. Phys. **2**, 253 (1998).
[9] I. Arsene *et al.* (BRAHMS Collaboration), Nucl. Phys. A **757**, 1 (2005).
[10] B. B. Back *et al.*, Nucl. Phys. A **757**, 28 (2005).
[11] K. Adcox *et al.* (PHENIX Collaboration), Nucl. Phys. A **757**, 184 (2005).
[12] M. Luzum and P. Romatschke, Phys. Rev. C **78**, 034915 (2008).
[13] H. Song and U. W. Heinz, J. Phys. G **36**, 064033 (2009).
[14] H. B. Meyer, Phys. Rev. D **76**, 101701 (2007).
[15] D. Kharzeev and K. Tuchin, J. High Energy Phys. 09 (2008) 093.
[16] F. Karsch, D. Kharzeev, and K. Tuchin, Phys. Lett. B **663**, 217 (2008).
[17] P. Arnold, G. D. Moore, and L. G. Yaffe, J. High Energy Phys. 05 (2003) 051.
[18] Z. Xu and C. Greiner, Phys. Rev. Lett. **100**, 172301 (2008).
[19] C. Wesp, A. El, F. Reining, Z. Xu, I. Bouras, and C. Greiner, Phys. Rev. C **84**, 054911 (2011).
[20] J. W. Chen, J. Deng, H. Dong, and Q. Wang, Phys. Rev. D **83**, 034031 (2011).
[21] S. Jeon, Phys. Rev. D **52**, 3591 (1995).
[22] S. Jeon and L. G. Yaffe, Phys. Rev. D **53**, 5799 (1996).
[23] M. E. Carrington, D. Hou, and R. Kobes, Phys. Rev. D **62**, 025010 (2000).
[24] E. Wang and U. W. Heinz, Phys. Lett. B **471**, 208 (1999).
[25] Y. Hidaka and T. Kunihiro, Phys. Rev. D **83**, 076004 (2011).
[26] J. S. Gagnon and S. Jeon, Phys. Rev. D **76**, 105019 (2007).
[27] U. W. Heinz, Ann. Phys. (NY) **161**, 48 (1985).

[28] H. T. Elze, M. Gyulassy, and D. Vasak, Nucl. Phys. B **276**, 706 (1986).
[29] T. S. Biro, E. van Doorn, B. Muller, M. H. Thoma, and X. N. Wang, Phys. Rev. C **48**, 1275 (1993).
[30] J. P. Blaizot and E. Iancu, Nucl. Phys. B **557**, 183 (1999).
[31] R. Baier, A. H. Mueller, D. Schiff, and D. T. Son, Phys. Lett. B **502**, 51 (2001).
[32] Q. Wang, K. Redlich, H. Stöcker, and W. Greiner, Phys. Rev. Lett. **88**, 132303 (2002).
[33] F. A. Berends, R. Kleiss, P. De Causmaecker, R. Gastmans, and T. T. Wu, Phys. Lett. B **103**, 124 (1981).
[34] R. K. Ellis and J. C. Sexton, Nucl. Phys. B **269**, 445 (1986).
[35] T. Gottschalk and D. W. Sivers, Phys. Rev. D **21**, 102 (1980).
[36] H. A. Weldon, Phys. Rev. D **26**, 1394 (1982).
[37] R. D. Pisarski, Phys. Rev. Lett. **63**, 1129 (1989).
[38] H. Heiselberg and X. N. Wang, Nucl. Phys. B **462**, 389 (1996).
[39] J. P. Blaizot, E. Iancu, and A. Rebhan, Phys. Rev. D **63**, 065003 (2001).
[40] J. O. Andersen, E. Braaten, E. Petitgirard, and M. Strickland, Phys. Rev. D **66**, 085016 (2002).
[41] S. Caron-Huot and G. D. Moore, Phys. Rev. Lett. **100**, 052301 (2008).
[42] J. W. Chen, H. Dong, K. Ohnishi, and Q. Wang, Phys. Lett. B **685**, 277 (2010).
[43] J. F. Gunion and G. Bertsch, Phys. Rev. D **25**, 746 (1982).
[44] S. K. Das and J. Alam, Phys. Rev. D **82**, 051502 (2010).
[45] S. K. Das and J. Alam, Phys. Rev. D **83**, 114011 (2011).
[46] R. Abir, C. Greiner, M. Martinez, and M. G. Mustafa, Phys. Rev. D **83**, 011501 (2011).
[47] T. Bhattacharyya, S. Mazumder, S. K. Das, and J. Alam, Phys. Rev. D **85**, 034033 (2012).
[48] M. Gyulassy, M. Plumer, M. Thoma, and X. N. Wang, Nucl. Phys. A **538**, 37C (1992).
[49] X.-N. Wang, M. Gyulassy, and M. Plumer, Phys. Rev. D **51**, 3436 (1995).
[50] P. Résibois and M. D. Leener, *Classical Kinetic Theory of Fluids* (Wiley, New York, 1977).
[51] G. Baym, H. Monien, C. J. Pethick, and D. G. Ravenhall, Phys. Rev. Lett. **64**, 1867 (1990).
[52] H. Heiselberg, Phys. Rev. D **49**, 4739 (1994).
[53] S. Weinberg, Astrophys. J. **168**, 175 (1971).
[54] J. W. Chen and E. Nakano, Phys. Lett. B **647**, 371 (2007).
[55] M. Prakash, M. Prakash, R. Venugopalan, and G. Welke, Phys. Rep. **227**, 321 (1993).
[56] A. Dobado and F. J. Llanes-Estrada, Phys. Rev. D **69**, 116004 (2004).
[57] A. Dobado and S. N. Santalla, Phys. Rev. D **65**, 096011 (2002).
[58] J. W. Chen, Y. H. Li, Y. F. Liu, and E. Nakano, Phys. Rev. D **76**, 114011 (2007).
[59] K. Itakura, O. Morimatsu, and H. Otomo, Phys. Rev. D **77**, 014014 (2008).
[60] H. B. Meyer, Nucl. Phys. A **830**, 641C (2009).
[61] A. Nakamura and S. Sakai, Phys. Rev. Lett. **94**, 072305 (2005).
[62] H. B. Meyer, Eur. Phys. J. A **47**, 86 (2011).
[63] Y. Hidaka and R. D. Pisarski, Phys. Rev. D **81**, 076002 (2010).
[64] M. Asakawa, S. A. Bass, and B. Muller, Phys. Rev. Lett. **96**, 252301 (2006).
[65] O. Kaczmarek and F. Zantow, Phys. Rev. D **71**, 114510 (2005).
[66] L. P. Csernai, J. I. Kapusta, and L. D. McLerran, Phys. Rev. Lett. **97**, 152303 (2006).
[67] M. Bluhm, B. Kampfer, and K. Redlich, Phys. Rev. C **84**, 025201 (2011).
[68] J.-W. Chen and J. Wang, Phys. Rev. C **79**, 044913 (2009).
[69] E. Lu and G. D. Moore, Phys. Rev. C **83**, 044901 (2011).
[70] D. Fernandez-Fraile and A. Gomez Nicola, Phys. Rev. Lett. **102**, 121601 (2009).
[71] A. Dobado, F. J. Llanes-Estrada, and J. M. Torres-Rincon, Phys. Lett. B **702**, 43 (2011).
[72] P. Chakraborty and J. I. Kapusta, Phys. Rev. C **83**, 014906 (2011).
[73] D. Davesne, Phys. Rev. C **53**, 3069 (1996).
[74] J. Noronha-Hostler, J. Noronha, and C. Greiner, Phys. Rev. Lett. **103**, 172302 (2009).
[75] K. Paech and S. Pratt, Phys. Rev. C **74**, 014901 (2006).
[76] H. B. Meyer, J. High Energy Phys. 04 (2010) 099.
[77] D. Teaney, Phys. Rev. D **74**, 045025 (2006).
[78] G. D. Moore and O. Saremi, J. High Energy Phys. 09 (2008) 015.
[79] P. Romatschke and D. T. Son, Phys. Rev. D **80**, 065021 (2009).
[80] H. B. Meyer, Phys. Rev. Lett. **100**, 162001 (2008).
[81] S. S. Gubser, A. Nellore, S. S. Pufu, and F. D. Rocha, Phys. Rev. Lett. **101**, 131601 (2008).
[82] B. C. Li and M. Huang, Phys. Rev. D **80**, 034023 (2009).
[83] R. A. Lacey *et al.*, Phys. Rev. Lett. **98**, 092301 (2007).
[84] J.-W. Chen, M. Huang, Y.-H. Li, E. Nakano, and D.-L. Yang, Phys. Lett. B **670**, 18 (2008).
[85] J.-W. Chen, C.-T. Hsieh, and H.-H. Lin, Phys. Lett. B **701**, 327 (2011).
[86] J.-W. Chen, M. Huang, C.-T. Hsieh, and H.-H. Lin, Phys. Rev. D **83**, 115006 (2011).
[87] A. Dobado, F. J. Llanes-Estrada, and J. M. Torres-Rincon, Phys. Rev. D **80**, 114015 (2009).
[88] D. Fernandez-Fraile, Phys. Rev. D **83**, 065001 (2011).